AGU100 ADVANCING EARTH AND SPACE SCIENCE

Geophysical Research Letters

RESEARCH LETTER
10.1029/2018GL078082

Key Points:
- We injected pressurized H_2O-, CO_2-, and H_2O + CO_2-rich fluids in unaltered and altered basalt-hosted preloaded faults
- Frictional instabilities occurred at similar fluid pressures and normal stresses independently of the degree of alteration of basalts and fluid composition
- Fast mineral carbonation occurred in basalt-hosted faults sheared in H_2O + CO_2-rich fluids

Supporting Information:
- Supporting Information S1
- Table S1
- Table S2
- Table S3

Correspondence to:
P. Giacomel,
piercarlo.giacomel@uniroma1.it

Citation:
Giacomel, P., Spagnuolo, E., Nazzari, M., Marzoli, A., Passelegue, F., Youbi, N., & Di Toro, G. (2018). Frictional instabilities and carbonation of basalts triggered by injection of pressurized H_2O- and CO_2-rich fluids. *Geophysical Research Letters*, *45*, 6032–6041. https://doi.org/10.1029/2018GL078082

Received 10 FEB 2016
Accepted 5 JUN 2018
Accepted article online 12 JUN 2018
Published online 29 JUN 2018

Frictional Instabilities and Carbonation of Basalts Triggered by Injection of Pressurized H_2O- and CO_2- Rich Fluids

Piercarlo Giacomel[1,2], Elena Spagnuolo[3], Manuela Nazzari[3,4], Andrea Marzoli[1], François Passelegue[5], Nasrrddine Youbi[6,7], and Giulio Di Toro[1,3]

[1]Dipartimento di Geoscienze, Università degli Studi di Padova, Padua, Italy, [2]Now at Dipartimento di Scienze della Terra, Sapienza Università di Roma, Rome, Italy, [3]Istituto Nazionale di Geofisica e Vulcanologia, Rome, Italy, [4]Dipartimento di Scienze della Terra, Sapienza Università di Roma, Rome, Italy, [5]LEMR, IIC, ENAC, EPFL, Lausanne, Switzerland, [6]Geology Department, Faculty of Sciences-Semlalia, Cadi Ayyad University, Marrakech, Morocco, [7]Instituto Dom Luiz, Faculdade de Ciências, Universidade de Lisboa, Lisbon, Portugal

Abstract The safe application of geological carbon storage depends also on the seismic hazard associated with fluid injection. In this regard, we performed friction experiments using a rotary shear apparatus on precut basalts with variable degree of hydrothermal alteration by injecting distilled H_2O, pure CO_2, and H_2O + CO_2 fluid mixtures under temperature, fluid pressure, and stress conditions relevant for large-scale subsurface CO_2 storage reservoirs. In all experiments, seismic slip was preceded by short-lived slip bursts. Seismic slip occurred at equivalent fluid pressures and normal stresses regardless of the fluid injected and degree of alteration of basalts. Injection of fluids caused also carbonation reactions and crystallization of new dolomite grains in the basalt-hosted faults sheared in H_2O + CO_2 fluid mixtures. Fast mineral carbonation in the experiments might be explained by shear heating during seismic slip, evidencing the high chemical reactivity of basalts to H_2O + CO_2 mixtures.

Plain Language Summary The injection of H_2O+CO_2 mixtures in basalts has been proposed for CO_2 storage as an appealing option to the injection of CO_2 fluids. In fact, H_2O+CO_2 fluids should react with basalts and induce the precipitation of carbonate minerals. The huge advantage of this storage technique is that, by *turning CO_2 into rock* (New York Times 9/2/2015), it prevents the risk of CO_2 leakage driven by buoyancy forces in the storage site. However, though it is well known that fluid injection may induce seismicity (e.g., Ellsworth, Science, 2013), the frictional behavior of faults in basalts injected by H_2O+CO_2 fluids is still poorly known. To provide insights on the induced-seismicity potential of this CO_2 storage technique, we reproduced the ambient conditions of typical H_2O+CO_2 storage sites by exploiting the rotary shear apparatus Slow to High Velocity Apparatus (INGV-Rome, Italy). Our experimental results show that fluid composition and degree of alteration of basalts had a negligible role in controlling the maximum fluid pressure that the experimental fault can sustain before failure. Evidences for mineral carbonation after the experiments sheared with CO_2-rich water attest the high chemical reactivity of basalts in acidic environment.

1. Introduction

Reducing the concentration of CO_2 in the atmosphere is among the greatest challenges of the present century. Large-scale carbon capture and geological storage have been proposed to reach this target (Bachu et al., 2007; Matter & Kelemen, 2009). One way to provide a long-lasting, thermodynamically stable, and environmentally benign carbon storage is through mineral carbonation (Oelkers et al., 2008). This process requires combining CO_2-rich water with dissolved divalent cations (primarily Ca^{2+}, Mg^{2+}, and Fe^{2+}) to precipitate carbonate minerals. The most efficient sources of divalent cations are silicate minerals like olivine, plagioclase, and pyroxenes, that is, the main constituents of basaltic rocks such as those of continental flood basalts. In particular, dissolution of CO_2 into water during its injection into basalt hosted reservoirs enhances the geological storage security compared to conventional geological formations, such as saline aquifers. In fact, injection of fully predissolved CO_2 mitigates the risks of fluid leakage driven by buoyancy forces back to the surface, so that injection could take place at shallower depth than those where CO_2 behaves as supercritical (usually $<$1,000 m, depending on the geothermal gradient; e.g., Edlmann et al., 2013). Moreover, CO_2-rich water interaction with pyroxene, olivine, etc., in basalts accelerates dissolution-carbonation reactions, thus mineral trapping (Aradóttir et al., 2012; Matter et al., 2016).

However, the amount of dissolved CO_2 at operative depths typical for carbon sequestration into basaltic aquifers (Alfredsson et al., 2013) is in the ratio 30–70 g CO_2 per kg H_2O (Choi & Nešić, 2011). Consequently, the large amounts of water to be injected during subsurface CO_2 storage efforts may trigger earthquakes in response to pore fluid overpressures in the vicinity of preexisting faults (Zoback & Gorelick, 2012). Specifically, injection of pressurized CO_2-rich fluids affects the shear strength of faults by (1) mechanical effects due to the increase in pore fluid pressure (Hubbert & Rubey, 1959) and (2) a variety of coupled chemically mediated mechanical processes, which may render faults more prone to frictional instabilities (Rohmer et al., 2016, and references therein for an overall overview). While the effect of water-rich fluids on fault reactivation has been studied extensively, the mechanical behavior of faults submitted to injections of CO_2-rich fluids as well as the effect of the degree of alteration of rocks on the dynamics of the onset of slip remains largely unknown. So far, most experimental studies have addressed the effects of the short-term (i.e., timescale of laboratory experiments: hours to days) and of the long-term (timescales over 100 years, up to 10 kyr) exposure to CO_2-rich water (brine) on the frictional properties of faults and fractures hosted in conventional sandstone reservoirs (Bakker et al., 2016; Samuelson & Spiers, 2012) and in anhydrite and claystone caprocks (e.g., Pluymakers et al., 2014). Nonetheless, a knowledge gap regarding the frictional behavior in shallower alternative CO_2 storage systems, involving injection of CO_2-rich water in basaltic reservoirs, still exists. Since hydrothermally altered basaltic rocks may be chosen as suitable CO_2 storage reservoirs, the study of the frictional behavior of basaltic rocks with variable degree of alteration in the presence of pressurized CO_2 and H_2O + CO_2 fluids is of paramount importance.

Here we investigated the role of H_2O- and CO_2-rich pressurized fluids on the triggering of frictional instabilities of preloaded experimental faults in basalts. The experiments were designed to reproduce the rock-type and the ambient conditions relevant for Hellisheidi (Iceland) CO_2-injection site (CarbFix pilot project: Gislason & Oelkers, 2014; Gislason et al., 2010). In fact, to date, this is the first storage site in which CO_2 is dissolved in H_2O before being injected in a basalt-built reservoir. The reservoir is located in a low-temperature geothermal area at ~500 m depth, corresponding to a lithostatic pressure of about 15 MPa, and at ~25°C ambient temperature (Alfredsson et al., 2013). Our results that could apply to other voluminous basaltic occurrences (e.g., continental flood basalts sequences) show that fault instability nucleation occurs regardless of the state of alteration of basalts and chemical composition of injection fluids.

2. Methods

2.1. Sample Selection and Petrography

Thick lava sequences pertaining to the Central Atlantic magmatic province (CAMP: Goldberg et al., 2010) or the Columbia River basalts (Wallula pilot project: McGrail et al., 2006, 2011) have been proposed as suitable CO_2-storage targets. Therefore, we selected representative samples of these two continental basalt provinces. For the CAMP, basaltic lava flows and shallow intrusions (sills) were collected in Morocco (Marzoli et al., 2004), eastern North America (Merle et al., 2014), and Portugal (Callegaro et al., 2014). The selected samples have an average grain size of 100–300 μm and a maximum grain size $<$2 mm. The main primary minerals of unaltered continental flood basalts are Ca-rich plagioclase (~45–50 vol %), clinopyroxene (augite and/or pigeonite, ~40–45 vol %), and Fe-Ti oxides (~5 vol %); some samples contain up to ~5 vol % of sideromelane glass. Since the rock-forming minerals of nonaltered basalts are water free, the loss on ignition content (LOI or the weight loss measured after heating the sample at 1000°C for 24 hr) is a good proxy of the abundance of breakdown products (smectite, sericite, etc.) and of the degree of alteration of the basalt. A systematic analysis of the LOI values revealed different alteration state of the selected basalts (Table S1 in the supporting information), as confirmed by the variable modal content of secondary minerals such as phyllosilicates (sericite, smectite, illite, and chlorite) deriving from alteration of plagioclase and pyroxenes, and from devitrification of sideromelane (optical microscope analysis and bulk X-ray powder diffraction; Figures S1 and S2), which amounts to ~50 vol % in the most altered specimens. Hereinafter, the basaltic rocks are referred to as "unaltered" when their LOI is below 1.7% wt and the amount of alteration minerals is less than 5% in volume, and *vice versa* as "altered" (see Figures S1 and S3 for details).

2.2. Experimental and Analytical Methods

To investigate the effect of short-term fluid-rock interaction on the mechanical behavior of basalt-built faults, 20 friction experiments were performed with the rotary shear apparatus SHIVA (Slow to High Velocity

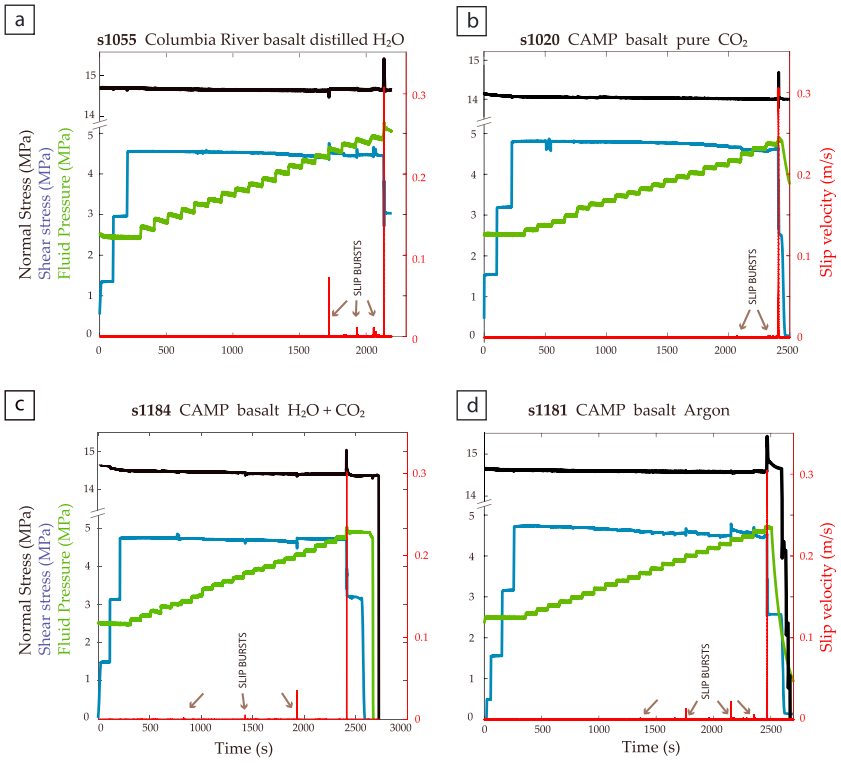

Figure 1. Experiments conducted under fluid pressure control at constant τ (blue in color curve) and σn (black curve) for (a) distilled H_2O, (b) pure CO_2, (c) H_2O + CO_2 mixture, and (d) pure argon. In all the experiments the *Pf* (green curve) was increased stepwise to trigger the main instability MI. Short lived slip bursts (grey arrows in the red curve), occurred before the onset of the MI. At MI the slip velocity was limited to 0.3 m/s.

Apparatus; Table S2) installed at the Istituto Nazionale di Geofisica e Vulcanologia in Rome (Italy; Di Toro et al., 2010; Niemeijer et al., 2011). The experiments were performed on hollow cylinders 30/50 mm internal/external diameter of the continental flood basalts described in section 2.1. The mineral and chemical compositions of the basalts were determined with X-ray powder diffraction (PANalytical X'Pert PRO) and X-ray fluorescence (WDS Philips PW2400) installed at Padua University. The effective porosity (<1%) was determined with a Helium-pycnometer Accu Pyc II 1340. Samples were jacketed in aluminum ring and embedded in epoxy to ensure the fluid pressure sealing as described in Nielsen et al. (2012). Bare surfaces were ground flat and parallel with a surface grinder to impose the same roughness on all sample assemblages (wavelength of ~50 μm and height of ~10 μm: e.g., Passelègue et al., 2016). This procedure ensures in most cases sample misalignment smaller than 100 μm once the rock specimens are installed in SHIVA. The sample pair was inserted in a vessel allowing pressurized fluid confinement (Figure S4; Violay et al., 2013, 2014). The injected fluids consisted of distilled H_2O, pure CO_2, pure argon, and a mixture of H_2O + CO_2. We used three different pressurizing circuits depending on the composition of the fluid (Text S1). Normal stress σ_n, fluid pressure *Pf*, axial shortening, equivalent slip δ, slip velocity *V*, and shear stress τ (determined on the annular samples; see Shimamoto & Tsutsumi, 1994) were acquired at a frequency up to 250 Hz. To assess the role of the chemistry of the injected fluids on the reactivation of faults juxtaposing basalts with variable degree of hydrothermal alteration, the frictional experiments were conducted over a range of σ_n from 10 to 20 MPa, at a starting fluid pressure Pf_i from 0.5 to 5 MPa. Injection of fluids initiated under a constant shear stress τ equal to 5 MPa (Table S2).

Notably, to approach the CarbFix reservoir working conditions, several tests were performed by applying σ_n = 15 MPa and an initial *Pf* = 2.5 MPa at room temperature (*T* ~ 20–25°C; Alfredsson et al., 2013). The experimental procedure consisted of the following steps: first we inserted the sample inside the pressure vessel and pumped the fluid to 0.1 MPa. Then we increased (1) σ_n up to target stress value $\sigma_{n,\,target}$; (2) *Pf* up to the starting fluid pressure Pf_i, under drained conditions (Text S1 and Figure S4); and (3) τ in three steps of 1.67 MPa every 100 s up to 5 MPa (Figure 1). After this stage, σ_n and τ were kept constant during the entire duration of the experiment (the recording rate of the inverter/controller feedback loop system used to control the

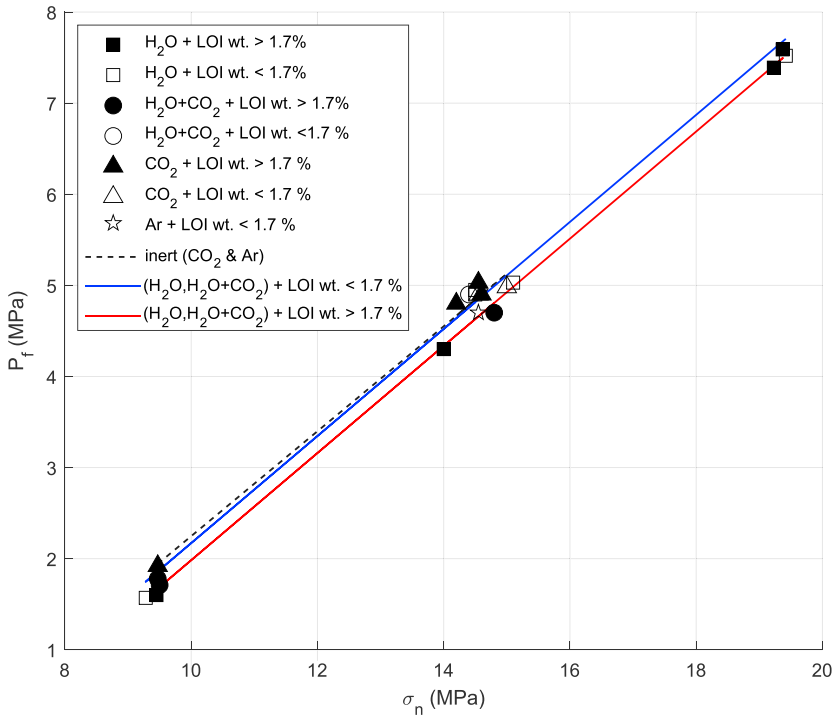

Figure 2. Dependence of the main frictional instability on the fluid pressure at a given normal stress, with fluid composition and LOI (wt %) content of the most altered samples of the fault pairs (i.e., the ones with the highest LOI; see section 3.1). The black, red, and blue best fit lines are obtained by linear regression of the plotted P_f MI-σ_n MI data of the experiments sheared in CO_2 and Ar, H_2O, and H_2O + CO_2 with LOI > 1.7%, and in H_2O and H_2O + CO_2 with LOI < 1.7%, respectively. Experimental errors are smaller than symbol size.

shear stress applied from the brushless engine was 16 kHz). Lastly, the *Pfi* was increased of ΔPf = 0.1 MPa every ~100 s to trigger the main fault instability resulting in a seismic slip event limited to V = 0.3 m/s. A time step of 100 s was sufficient to guarantee fluid penetration within the entire fault slipping zone (Spagnuolo et al., 2018).

3. Results

3.1. Mechanical Data

In Figure 1 we report the evolution of the σ_n, *Pf*, τ, and V with time during experiments conducted with the different fluids tested (H_2O, CO_2, H_2O + CO_2, and argon in respectively Figures 1a–1d). Before the main instability, the stepwise *Pf* increase resulted in the onset of short-lived spontaneous slip bursts (grey arrows in Figure 1) with V ranging from 10^{-3} m/s up to 0.3 m/s at the main instability. Slower slip rate burst events ($V < 10^{-3}$ m/s), if present, were not distinguishable from the background noise and creep. The precursory slip bursts resulted in minor shear stress drops ($\Delta\tau < 0.2$ MPa) followed by fault restrengthening (Figure 1). The experiment ended with the main frictional instability, or the slip event during which the fault strength dropped rapidly and accelerates up to 0.3 m/s due to the onset of macroscopic fault reactivation. The fluid pressure and normal stress at the onset of the main instability were defined as Pf_{MI} and σ_{nMI}, respectively, and are shown in Table S2 and Figure 2 for all conditions tested.

We tested the dependence of the frictional properties from (1) the degree of alteration of rocks and (2) fluid composition, by combining basalts with variable LOI wt % content in the experimental fault pair. Moreover, as altered minerals (smectite, etc.) and glass have a lower indentation hardness than primary rock-forming minerals (Beeler et al., 2008), we tested the hypothesis that the most altered sample (i.e., the one with the highest LOI) of each pair determines the macroscopic properties of the experimental fault. Accordingly, we defined basalt-faults as unaltered when the LOI of the most altered samples of the fault pairs is below 1.7% wt and altered for LOI > 1.7% wt.

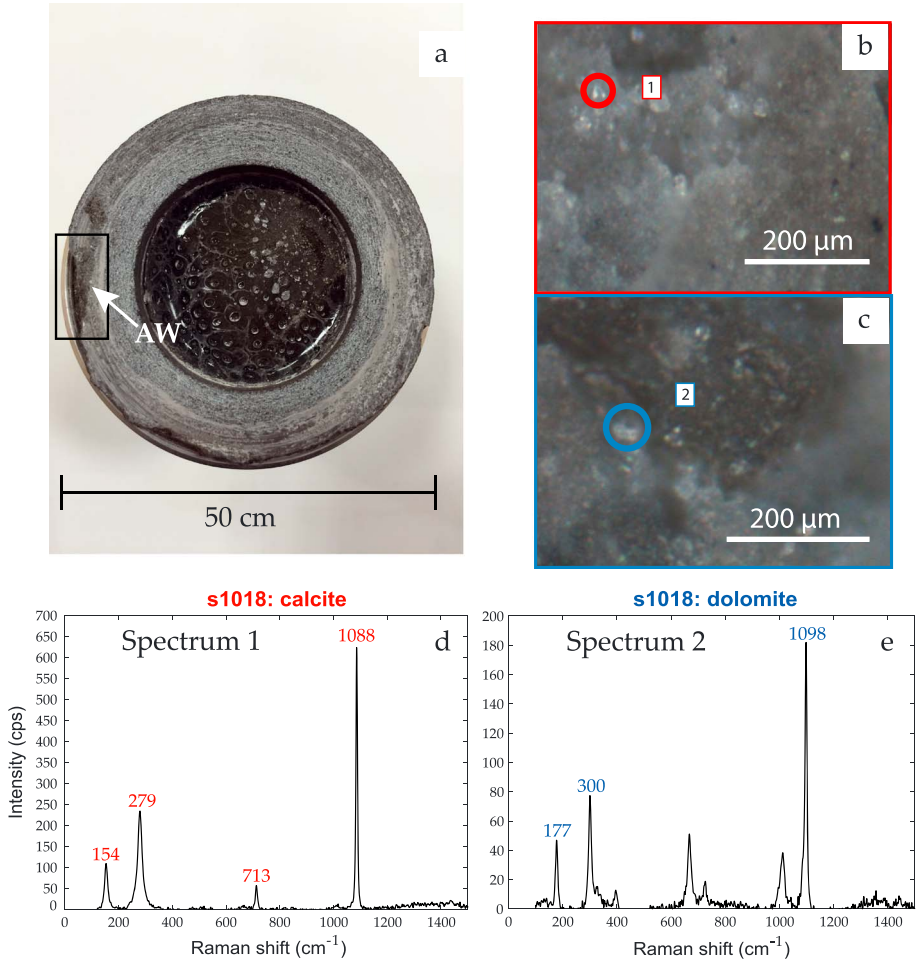

Figure 3. Cohesive slip surfaces of the experimental faults and evidence of carbonation of basalts. (a) Slip surface of a basalt sheared in $H_2O + CO_2$ mixture. Evidence of adhesive wear (AW, white arrow). During frictional sliding, especially at 0.3 m/s, wear debris remained welded to the slip surfaces. (b and c) Close up of the slip surface with calcite and dolomite microcrystals (Raman microprobe image). (d and e) Raman spectra of microcrystals of calcite and dolomite. Numbers are the characteristic intensity micro-Raman peaks of the two minerals.

Independently of the tested environmental conditions (i.e., initial state of stress, nature of the fluids, and degree of alteration), fault reactivation follows the Terzaghi's principle (Terzaghi, 1925). The larger the normal stress acting on the experimental fault, the larger the fluid pressure required to trigger the main frictional instability (Table S2 and Figure 2). All the experimental data, with few exceptions, fell within a narrow band delimited by two straight parallel best fit lines in the Pf_{MI}-$\sigma_{n\ MI}$ space (Figure 2). The blue and red lines are the trends associated to unaltered and altered basalt-built faults, respectively, sheared either in distilled H_2O or $H_2O + CO_2$, whereas the black dashed best fit line refers to all the experimental faults (independently of their LOI wt % content), interacting with pure CO_2 or Ar. The best fit lines arise from a linear regression analysis, and their high R^2 values (0.987–0.999) reflect the low scatter of the experimental data and the robustness of the fits. Two observations arise: (1) the blue straight line almost overlaps with the black line in the σ_n range 9–15 MPa, attesting that unaltered basalt-built faults sheared in H_2O and $H_2O + CO_2$ reactivate at comparable fluid pressures as in the case of basalts pressurized with pure CO_2 or Ar, and (2) for a given normal stress at main instability, unaltered and altered basalt-built faults flooded with H_2O and $H_2O + CO_2$, reactivate at comparable fluid pressures (the Pf_{MI} difference between the red and blue best fit trends is ~0.3 MPa). Therefore, data analysis clearly points to similar mechanical behavior in the experiments conducted on basalts sheared in CO_2, H_2O, and $H_2O + CO_2$ mixtures, independently of the fluid chemistry and the alteration state of basalts.

3.2. Microstructural and Microanalytical Data

The slipping zone of all the sheared samples consisted of lineated principal slip surfaces overlaying <100 μm thick gouge layers. However, in the experiments performed in the presence of water-rich fluids, only cohesive gouge was preserved after the tests, as most of the gouge layer was flushed away during the sample recovery. The slipping zone resulted from abrasive and adhesive wear of the basalts during sliding (Figure 3a). Systematic micro-Raman investigation of the slipping fault patches interested by grain size reduction and adhesive wearing, evidenced the occurrence of micrometric crystals of dolomite only in the case of basalts sheared in $H_2O + CO_2$ fluids (Figures 3b–3e). Ion-chromatography analysis showed that given the similar degree of alteration of the basalts, fluids recovered after experiments performed with $H_2O + CO_2$ mixtures had higher concentration of Mg^{2+} compared to the fluids from experiments with distilled H_2O (e.g., s1055 versus s1184; Table S3). Since both fault sides contribute to cation release during shearing, the composition of the recovered fluid was related to the average of the LOI content of the sample pair forming the experimental fault.

4. Discussion

4.1. Main Frictional Instability: Role of Fluid Composition and Degree of Alteration of Basalts

We performed friction experiments that enabled us to get better insights on the effects of the short-term exposure of H_2O- and CO_2-rich fluids with variably hydrothermally altered basalt-built preloaded faults. Clay minerals like smectite and illite and other phyllosilicates are the typical breakdown products of altered basalt. Their mechanical (e.g., pore fluid pressure) and chemical (e.g., subcritical crack growth and water adsorption) interaction with fluids is expected to reduce the fault frictional strength (Moore & Lockner, 2007; Remitti et al., 2015; Wintsch et al., 1995).

Notably, the similar response of basalts sheared with CO_2 independently of their degree of alteration at a given σ_{nMI} suggests that pure CO_2 has mainly a mechanical effect in triggering the main instability (Figure 2). This hypothesis is consistent with Wang et al. (2013), who observed the lack of chemical reactions following anhydrous CO_2-rock interaction, and is strengthened by the test performed with Ar, which lies in the same P_{fMI}-σ_{nMI} field as in the experiments pressurized with pure CO_2. Moreover, the best fit line for the occurrence of the main frictional instabilities for unaltered basalt-hosted faults sheared in pressurized H_2O or $H_2O + CO_2$ overlaps with the one resulting from the injection of CO_2 and Ar, suggesting that fault reactivation is mainly due to the mechanical role of the fluids (Figure 2). The triggering of the main frictional instabilities for altered basalt-hosted faults sheared in the presence of pressurized H_2O or $H_2O + CO_2$ required, under a given normal stress, a fluid pressure on average 0.3 MPa smaller than the one required for the unaltered samples. The offset between the two best fit lines for the main frictional instabilities for unaltered or altered faults is within the reproducibility range of laboratory data. The scatter of the experimental data could be ascribed to local heterogeneities in mineral composition and rock microstructure, as well as micrometric sample misalignments. In fact, though the samples are carefully prepared (see details in Nielsen et al., 2012), misalignments up to 100 μm between the sample pairs are extremely difficult to eliminate in quite hard rocks as basalts. Consequently, the experimental data set reported here suggests that the chemically mediated mechanical fault weakening due to short-term exposure to $H_2O + CO_2$ fluids can be ruled out, as the main instabilities occur at similar fluid pressures independently of the composition of the injected fluids and of the degree of alteration of the basalts.

This conclusion is akin to findings from Samuelson and Spiers (2012), aimed at investigating the short-term impact of CO_2 exposure on the mechanical behavior of wet simulated quartz- and clay-rich gouges, whereas analogous experiments in wet-anhydrite fault gouges evidenced additional CO_2-weakening effects to that caused by water alone (Pluymakers et al., 2014). Instead, despite the high chemical reactivity of basalt-forming minerals in acidic environment as attested by the chemistry of the recovered fluids (Table S3), the presence of $H_2O + CO_2$-rich fluids did not entail macroscopic variations in frictional strength of faults.

Furthermore, phyllosilicates content had no significant influence on the frictional strength of the basalt-hosted faults. Unfortunately, because of the design of the pressure vessel, the gouges in the slipping zones could not be recovered because flushed away with water during sample recovery. This impeded detailed microstructural analysis of the entire slipping zone. However, we argue that phyllosilicates did not form a

continuous weak layer. Instead, it seems reasonable that faults accommodated deformation predominantly by cataclastic processes in all the experiments.

4.2. Carbonation Reactions

Newly formed dolomite grains were found only in cohesive slipping zones recovered from experiments performed in $H_2O + CO_2$ mixtures (Figure 3), in contrast to calcite crystals that were present in limited amounts in the starting protolith as vacuole fillings. Basalt carbonation is the result of kinetic processes involving (1) dissolution of basalt primary minerals due to interaction with acid water, (2) diffusion of the dissolved material, and (3) precipitation of carbonates. The rate-limiting step in mineral sequestration is associated to alkali earth ions availability, released from the parent minerals. Because Ca-rich clinopyroxene is the sustaining contributor of divalent cations during dissolution of basalts (Wells et al., 2017), we argue that dolomite (and possibly calcite) precipitation during the $H_2O + CO_2$ tests is the result of the following reactions (Gislason et al., 2010; Aradóttir et al., 2011):

$$CO_{2\ (aq)} + H_2O_{(l)} = H_2CO_{3\ (l)} = HCO_3^- + H^+ = CO_3^{\ 2} - +2H^+ \quad \text{(hydration and dissociation)} \quad (1)$$

$$\underset{\text{Clinopyroxene}}{(Ca, Mg, Fe)_2SiO_{3(s)}} + 2H^+ = 2(Ca, Mg, Fe)^{2+} + SiO_{2(aq)} + H_2O_{(l)} \quad \text{(dissolution)} \quad (2)$$

$$(Mg, Ca)^{2+} + CO_{2(aq)} + H_2O_{(l)} = \underset{\text{Carbonate minerals}}{(Mg, Ca)CO_{3(s)}} + 2H^+ \quad \text{(precipitation)} \quad (3)$$

According to equation (1), Ca^{2+} and Mg^{2+}, leached mainly from Ca-rich clinopyroxene in acid environment (equation (2)), react with CO_2 to precipitate calcite and dolomite (equation (3)). Notably, the acid environment of $H_2O + CO_2$ mixtures (pH ≃ 3.2 at Pf = 2.5–5 MPa and 20 < T < 30°C, from Diamond & Akinfiev, 2003; Figure S5) promotes the release of Mg^{2+} from rock-forming basaltic minerals as showed by comparing the geochemical analysis of $H_2O + CO_2$ and distilled H_2O in basalts with similar mean LOI and cumulated slip (cf. s1055 and s1184; Table S3). This is corroborated by the higher Mg^{2+} concentration leached by more altered samples sheared in $H_2O + CO_2$ mixtures that cumulated less displacement than their counterpart with lower mean LOI and pressurized with only water (s1018 versus s1021; Table S3). Moreover, as CO_2-dissolution into water can occur within 5 min during the CO_2 injection process (Sigfusson et al., 2015), and the experiments last less than 1 hr, cation enrichment in solution during the stage preceding the main instability is expected to occur.

Finally, since carbonate mineral solubility decreases with increasing temperature (Langmuir, 1997), reaction in equation (3) could be favored by the temperature increase due to the frictional heat exchanged in the slipping zone during the episodic slip bursts, and especially after the main instability was achieved and the pair sample sheared at V = 0.3 m/s. The latter, together with the reduced grain size, would enhance significantly the kinetics of dissolution of basalt rock-forming minerals and precipitation of calcite and dolomite from the solution $H_2O + CO_2$ despite the relatively short duration of the experiment (<40 min in total).

Following the reasoning in Kelemen et al. (2011), assuming that basalt mineral carbonation rates are comparable to olivine carbonation rates, the optimum temperature for equation (4) would be in the range 150–200°C (Kelemen & Matter, 2008). This is in good agreement with the bulk temperature increase estimated along the slipping zone at the main frictional instability. If the heat production is (Beeler et al., 2008; Lachenbruch & Sass, 1980)

$$dQ = \tau\, V\, dt \quad (4)$$

an estimate of the bulk temperature increase in the slipping zone during the experiments can be computed numerically using the approximation (Carslaw & Jaeger, 1959; Nielsen et al., 2008; Figure S6) $T(t) = \frac{1}{\rho \cdot C_p \cdot \sqrt{\kappa\pi}} \cdot \int_0^t \frac{1}{2} \cdot \frac{Q}{\sqrt{t-t'}}\, dt$ (with, for basalts, thermal diffusivity κ = 0.012 cm^2/s; Hanley et al., 1978), specific heat capacity Cp = 898 $J \cdot kg^{-1} \cdot K^{-1}$ (Waples & Waples, 2004), and density ρ = 2,960 kg/m^3). The numerical solution revealed indeed the achievement of bulk temperatures of several hundred degrees Celsius once the main instability was triggered, as shown in Figure S6. In small fault patches (<1 mm^2) of the experimental fault, because of flash heating at the asperity scale or of debris trapped in the slipping zone, temperatures can be higher than 1000°C (see Tisato et al., 2012, for discussion). This can also be attested by the presence of

adhesive wear products, because of frictional welding between opposing asperities in the slipping zone in all the experiments and independently of the composition of the injected fluid (Figure 3a). Adhesive wear products were also found in experiments performed with H_2O-rich fluids, suggesting the achievement of high temperatures despite the presence of water that should buffer the temperature increase (Violay et al., 2014). Furthermore, since thermal decomposition of dolomite and calcite happens at a temperature ranging from 600 to 800°C, this temperature interval can be reasonably regarded as an upper bound of the temperature reached in the slipping zone at the main frictional instability (Rodriguez-Navarro et al., 2009, 2012).

The presence of newly formed dolomite grains at the end of our friction experiments supports the great effectiveness of mineral carbonation in basalts interacting with $H_2O + CO_2$ mixtures (e.g., Aradóttir et al., 2012; Matter et al., 2016). However, in our experiments and compared to natural conditions, dolomite precipitation was possibly fostered by both rapid temperature rise (up to 600–800°C) and grain comminution associated to the main fault frictional instability and simulated seismic slip. In nature, if mineral precipitation associated to seismic slip would lead to significant fault clogging, buildup of fluid pressure may occur in the vicinity of the fault, further increasing the seismic hazard.

5. Conclusions

We investigated the effects of the injection of pressurized fluids (Ar, CO_2, H_2O, and $H_2O + CO_2$) in preloaded basalt-built experimental faults (Figure 1). Experimental conditions were designed to reproduce the typical operating conditions for CO_2 storage in basaltic-built reservoirs. The pressure of the fluid to trigger the main instability scaled linearly with the normal stress acting on the fault (Figure 2). Fluid composition and degree of alteration of basalts had a negligible role in controlling the maximum fluid pressure that the experimental fault could sustain before failure (i.e., main instability; Figure 2). In fact, more altered basalts (i.e., with higher LOI and higher content of secondary minerals such as sericite, smectite, etc.) sheared in H_2O- and $H_2O + CO_2$-rich fluids were just slightly more prone to the main frictional instability than less altered basalts and basalts sheared in pure CO_2 and Ar (Figure 2). However, this tiny discrepancy may be due to local heterogeneities in mineral composition and microstructure of basaltic samples.

The evidence of newly formed dolomite grains in the slipping zones of all the basalts (i.e., independently of the alteration state) sheared in $H_2O + CO_2$ mixtures is the result of the easy release of Ca^{2+} and Mg^{2+} from basalt-bearing minerals, plus grain size reduction and heat production during frictional sliding (Figure 3). The experiments discussed here confirm that dissolution and mineral carbonation of basalts in the presence of $H_2O + CO_2$ mixtures is extremely efficient, also during frictional sliding at seismic slip rates (~0.3 m/s) associated to the main instability event.

Acknowledgments
This work was funded by the European Research Council Project 614705 NOFEAR. Experimental and microanalytical data are available at GFZ Data Services (Giacomel et al., 2018: http://doi.org/10.5880/fidgeo.2018.013). We thank L. Tauro, E. Masiero, L. Peruzzo F. Zorzi, D. Pasqual, L.W. Kuo, F. Prando, and D. Cinti for technical support and analysis and P. McGrail for providing Columbia River basalt samples. We thank the Editor, N. Brantut, A. Pluymakers, and an anonymous reviewer for their constructive comments that improved remarkably our study.

References

Alfredsson, H. A., Oelkers, E. H., Hardarsson, B. S., Franzson, H., Gunnlaugsson, E., & Gislason, S. R. (2013). The geology and water chemistry of the Hellisheidi, SW-Iceland carbon storage site. *International Journal of Greenhouse Gas Control*, *12*, 399–418. https://doi.org/10.1016/j.ijggc.2012.11.019

Aradóttir, E. S. P., Sigurdardottir, H., Sigfusson, B., & Gunnlaugsson, E. (2011). CarbFix: A CCS pilot project imitating and accelerating natural CO_2 sequestration. *Greenh Gases*, *1*(2), 105–118. https://doi.org/10.1002/ghg.18

Aradóttir, E. S. P., Sonnenthal, E. L., Björnsson, G., & Jónsson, H. (2012). Multidimensional reactive transport modeling of CO_2 mineral sequestration in basalts at the Hellisheidi geothermal field, Iceland. *International Journal of Greenhouse Gas Control*, *9*, 24–40. https://doi.org/10.1016/j.ijggc.2012.02.006

Bachu, S., Bonijoly, D., Bradshaw, J., Burruss, R., Holloway, S., Christensen, N. P., & Mathiassen, O. M. (2007). CO_2 storage capacity estimation: Methodology and gaps. *International Journal of Greenhouse Gas Control*, *1*(4), 430–443. https://doi.org/10.1016/s1750-5836(07)00086-2

Bakker, E., Hangx, S. J., Niemeijer, A. R., & Spiers, C. J. (2016). Frictional behaviour and transport properties of simulated fault gouges derived from a natural CO_2 reservoir. *International Journal of Greenhouse Gas Control*, *54*, 70–83. https://doi.org/10.1016/j.ijggc.2016.08.029

Beeler, N. M., Tullis, T. E., & Goldsby, D. L. (2008). Constitutive relationships and physical basis of fault strength due to flash heating. *Journal of Geophysical Research*, *113*, B01401. https://doi.org/10.1029/2007JB004988

Callegaro, S., Rapaille, C., Marzoli, A., Bertrand, H., Chiaradia, M., Reisberg, L., et al. (2014). Enriched mantle source for the Central Atlantic magmatic province: New supporting evidence from southwestern Europe. *Lithos*, *188*, 15–32. https://doi.org/10.1016/j.lithos.2013.10.021

Carslaw, H., & Jaeger, J. (1959). *Heat in solids*. Oxford: Clarendon Press.

Choi, Y.-S., & Nešić, S. (2011). Determining the corrosive potential of CO_2 transport pipeline in high pCO_2–water environments. *International Journal of Greenhouse Gas Control*, *5*(4), 788–797. https://doi.org/10.1016/j.ijggc.2010.11.008

Di Toro, G., Niemeijer, A., Tripoli, A., Nielsen, S., Di Felice, F., Scarlato, P., et al. (2010). From field geology to earthquake simulation: A new state-of-the-art tool to investigate rock friction during the seismic cycle (SHIVA). *Rendiconti Lincei*, *21*(S1), 95–114. https://doi.org/10.1007/s12210-010-0097-x

Diamond, L. W., & Akinfiev, N. N. (2003). Solubility of CO_2 in water from −1.5 to 100°C and from 0.1 to 100 MPa: Evaluation of literature data and thermodynamic modelling. *Fluid Phase Equilibria*, *208*(1–2), 265–290. https://doi.org/10.1016/S0378-3812(03)00041-4

Edlmann, K., Haszeldine, S., & McDermott, C. I. (2013). Experimental investigation into the sealing capability of naturally fractured shale caprocks to supercritical carbon dioxide flow. *Environmental Earth Sciences*, *70*(7), 3393–3409. https://doi.org/10.1007/s12665-013-2407-y

Giacomel, P., Spagnuolo, E., Nazzari, M., Marzoli, A., Passelegue, F., Youbi, N., & Di Toro, G. (2018). Frictional and microanalytical data of basalts sheared with pressurized H_2O- and CO_2-rich fluids. GFZ Data Services. https://doi.org/10.5880/fidgeo.2018.013

Gislason, S. R., & Oelkers, E. H. (2014). Carbon storage in basalt. *Science*, *344*(6182), 373–374. https://doi.org/10.1126/science.1250828

Gislason, S. R., Wolff-Boenisch, D., Stefansson, A., Oelkers, E. H., Gunnlaugsson, E., Sigurdardottir, H., et al. (2010). Mineral sequestration of carbon dioxide in basalt: A pre-injection overview of the CarbFix project. *International Journal of Greenhouse Gas Control*, *4*(3), 537–545. https://doi.org/10.1016/j.ijggc.2009.11.013

Goldberg, D. S., Kent, D. V., & Olsen, P. E. (2010). Potential on-shore and off-shore reservoirs for CO_2 sequestration in Central Atlantic magmatic province basalts. *Proceedings of the National Academy of Sciences of the United States of America*, *107*(4), 1327–1332. https://doi.org/10.1073/pnas.0913721107

Hanley, E., Dewitt, D., & Roy, R. (1978). The thermal diffusivity of eight well-characterized rocks for the temperature range 300–1000 K. *Engineering Geology*, *12*, 31–47. https://doi.org/10.1016/0013-7952(78)90003-0

Hubbert, M. K., & Rubey, W. W. (1959). Role of fluid pressure in mechanics of overthrust faulting I. Mechanics of fluid-filled porous solids and its application to overthrust faulting. *Geological Society of America Bulletin*, *70*(2), 115–166.

Kelemen, P. B., & Matter, J. (2008). In situ carbonation of peridotite for CO_2 storage. *Proceedings of the National Academy of Sciences of the United States of America*, *105*(45), 17,295–17,300. https://doi.org/10.1073/pnas.0805794105

Kelemen, P. B., Matter, J., Streit, E. E., Rudge, J. F., Curry, W. B., & Blusztajn, J. (2011). Rates and mechanisms of mineral carbonation in peridotite: Natural processes and recipes for enhanced, in situ CO_2 capture and storage. *Annual Review of Earth and Planetary Sciences*, *39*(1), 545–576. https://doi.org/10.1146/annurev-earth-092010-152509

Lachenbruch, A. H., & Sass, J. H. (1980). Heat flow and energetics of the San Andreas Fault zone. *Journal of Geophysical Research*, *85*, 6185–6222. https://doi.org/10.1029/JB085iB11p06185

Langmuir, D. (1997). Aqueous environmental geochemistry (no. 551.48 L3.).

Marzoli, A., Bertrand, H., Knight, K. B., Cirilli, S., Buratti, N., Vérati, C., et al. (2004). Synchrony of the Central Atlantic magmatic province and the Triassic-Jurassic boundary climatic and biotic crisis. *Geology*, *32*(11), 973. https://doi.org/10.1130/g20652.1

Matter, J. M., & Kelemen, P. B. (2009). Permanent storage of carbon dioxide in geological reservoirs by mineral carbonation. *Nature Geoscience*, *2*(12), 837–841. https://doi.org/10.1038/ngeo683

Matter, J. M., Stute, M., Snæbjörnsdottir, S. Ó., Oelkers, E. H., Gislason, S. R., Aradottir, E. S., et al. (2016). Rapid carbon mineralization for permanent disposal of anthropogenic carbon dioxide emissions. *Science*, *352*(6291), 1312–1314. https://doi.org/10.1126/science.aad8132

McGrail, F. A., Spane, E. C., Sullivan, D. H. B., & Hund, G. (2011). The Wallula basalt sequestration pilot project. *Energy Procedia*, *4*, 5653–5660. https://doi.org/10.1016/j.egypro.2011.02.557

McGrail, H., Schaef, T., Ho, A. M., Chien, Y.-J., Dooley, J. J., & Davidson, C. L. (2006). Potential for carbon dioxide sequestration in flood basalts. *Journal of Geophysical Research*, *111*, B12201. https://doi.org/10.1029/2005JB004169

Merle, R., Marzoli, A., Reisberg, L., Bertrand, H., Nemchin, A., Chiaradia, M., et al. (2014). Sr, Nd, Pb and Os isotope systematics of CAMP Tholeiites from eastern North America (ENA): Evidence of a subduction-enriched mantle source. *Journal of Petrology*, *55*(1), 133–180. https://doi.org/10.1093/petrology/egt063

Moore, D. E., & Lockner, D. A. (2007). Friction of the smectite clay montmorillonite. In T. Dixon & C. Moore (Eds.), *The seismogenic zone of subduction thrust faults* (pp. 317–345). Columbia University Press.

Nielsen, S., Di Toro, G., Hirose, T., & Shimamoto, T. (2008). Frictional melt and seismic slip. *Journal of Geophysical Research*, *113*, B01308. https://doi.org/10.1029/2007JB005122

Nielsen, S., Spagnuolo, E., & Violay, M. (2012). Composite sample mount assembly (SAMOA): The ultimate sample preparation for rotary shear experiments. (Tech. Rep. 215). Istituto Nazionale di Geofisica e Vulcanologia.

Niemeijer, A., Di Toro, G., Nielsen, S., & Di Felice, F. (2011). Frictional melting of gabbro under extreme experimental conditions of normal stress, acceleration, and sliding velocity. *Journal of Geophysical Research*, *116*, B07404. https://doi.org/10.1029/2010JB008181

Oelkers, E. H., Gislason, S. R., & Matter, J. (2008). Mineral carbonation of CO_2. *Elements*, *4*(5), 333–337. https://doi.org/10.2113/gselements.4.5.333

Passelègue, F., Spagnuolo, E., Violay, M., Nielsen, S., Di Toro, G., & Schubnel, A. (2016). Frictional evolution, acoustic emissions activity, and off-fault damage in simulated faults sheared at seismic slip rates. *Journal of Geophysical Research: Solid Earth*, *121*, 7490–7513. https://doi.org/10.1002/2016JB012988

Pluymakers, A. M., Samuelson, J. E., Niemeijer, A. R., & Spiers, C. J. (2014). Effects of temperature and CO_2 on the frictional behavior of simulated anhydrite fault rock. *Journal of Geophysical Research: Solid Earth*, *119*, 8728–8747. https://doi.org/10.1002/2014JB011575

Remitti, F., Smith, S. A. F., Mittempergher, S., Gualtieri, A. F., & Di Toro, G. (2015). Frictional properties of fault zone gouges from the J-FAST drilling project (Mw 9.0 2011 Tohoku-Oki earthquake). *Geophysical Research Letters*, *42*, 2691–2699. https://doi.org/10.1002/2015GL063507

Rodriguez-Navarro, C., Kudlacz, K., & Ruiz-Agudo, E. (2012). The mechanism of thermal decomposition of dolomite: New insights from 2D-XRD and TEM analyses. *American Mineralogist*, *97*(1), 38–51. https://doi.org/10.2138/am.2011.3813

Rodriguez-Navarro, C., Ruiz-Agudo, E., Luque, A., Rodriguez-Navarro, A. B., & Ortega-Huertas, M. (2009). Thermal decomposition of calcite: Mechanisms of formation and textural evolution of CaO nanocrystals. *American Mineralogist*, *94*(4), 578–593. https://doi.org/10.2138/am.2009.3021

Rohmer, J., Pluymakers, A., & Renard, F. (2016). Mechano-chemical interactions in sedimentary rocks in the context of CO_2 storage: Weak acid, weak effects? *Earth-Science Reviews*, *157*, 86–110. https://doi.org/10.1016/j.earscirev.2016.03.009

Samuelson, J., & Spiers, C. J. (2012). Fault friction and slip stability not affected by CO_2 storage: Evidence from short-term laboratory experiments on North Sea reservoir sandstones and caprocks. *International Journal of Greenhouse Gas Control*, *11*, S78–S90. https://doi.org/10.1016/j.ijggc.2012.09.018

Shimamoto, T., & Tsutsumi, A. (1994). A new rotary-shear high-speed frictional testing machine: Its basic design and scope of research (in Japanese with English abstract). *Journal of Tectonic Research Group of Japan*, *39*, 65–78.

Sigfusson, B., Gislason, S. R., Matter, J. M., Stute, M., Gunnlaugsson, E., Gunnarsson, I., et al. (2015). Solving the carbon-dioxide buoyancy challenge: The design and field testing of a dissolved CO_2 injection system. *International Journal of Greenhouse Gas Control*, *37*, 213–219. https://doi.org/10.1016/j.ijggc.2015.02.022

Spagnuolo E., Violay M., Nielsen S., Cornelio C., & Di Toro G. (2018). Frictional instability under fluid stimulation: Insights from load-controlled experiments on preexisting faults. SEG, Lausanne, Switzerland, 25–28 September 2018.

Terzaghi, K. (1925). *Erdbaumechanik auf Bodenphysikalischer Grundlage*. Liepzig-Vienna: Franz Deuticke.
Tisato, N., Di Toro, G., Di Rossi, N., Quaresimin, M., & Candela, T. (2012). Experimental investigation of flash weakening in limestone. *Journal of Structural Geology*, *38*, 183–199. https://doi.org/10.1016/j.jsg.2011.11.017
Violay, M., Nielsen, S., Gibert, B., Spagnuolo, E., Cavallo, A., Azais, P., et al. (2014). Effect of water on the frictional behavior of cohesive rocks during earthquakes. *Geology*, *42*(1), 27–30. https://doi.org/10.1130/G34916.1
Violay, M., Nielsen, S., Spagnuolo, E., Cinti, D., Di Toro, G., & Di Stefano, G. (2013). Pore fluid in experimental calcite-bearing faults: Abrupt weakening and geochemical signature of co-seismic processes. *Earth and Planetary Science Letters*, *361*, 74–84. https://doi.org/10.1016/j.epsl.2012.11.021
Wang, X., Alvarado, V., Swoboda-Colberg, N., & Kaszuba, J. P. (2013). Reactivity of dolomite in water-saturated supercritical carbon dioxide: Significance for carbon capture and storage and for enhanced oil and gas recovery. *Energy Conversion and Management*, *65*, 564–573. https://doi.org/10.1016/j.enconman.2012.07.024
Waples, D. W., & Waples, J. S. (2004). A review and evaluation of specific heat capacities of rocks, minerals, and subsurface fluids. Part 1: Minerals and nonporous rocks. *Natural Resources Research*, *13*(2), 97–122. https://doi.org/10.1023/B:NARR.0000032647.41046.e7
Wells, R. K., Xiong, W., Giammar, D., & Skemer, P. (2017). Dissolution and surface roughening of Columbia River flood basalt at geologic carbon sequestration conditions. *Chemical Geology*, *467*, 100–109. https://doi.org/10.1016/j.chemgeo.2017.07.028
Wintsch, R. P., Christoffersen, R., & Kronenberg, A. K. (1995). Fluid-rock reaction weakening of fault zones. *Journal of Geophysical Research*, *100*, 13,021–13,032. https://doi.org/10.1029/94JB02622
Zoback, M. D., & Gorelick, S. M. (2012). Earthquake triggering and large-scale geologic storage of carbon dioxide. *Proceedings of the National Academy of Sciences of the United States of America*, *109*(26), 10,164–10,168. https://doi.org/10.1073/pnas.1202473109